**Wireless Networks manuscript No.**
(will be inserted by the editor)

# Cooperative Signal Amplification for Molecular Communication in Nanonetworks

**Sergi Abadal · Ignacio Llatser · Eduard Alarcón · Albert Cabellos-Aparicio**

Received: date / Accepted: date

**Abstract** Nanotechnology is enabling the development of devices in a scale ranging from a few to hundreds of nanometers. Communication between these devices greatly expands the possible applications, increasing the complexity and range of operation of the system. In particular, the resulting nanocommunication networks (or nanonetworks) show great potential for applications in the biomedical field, in which diffusion-based molecular communication is regarded as a promising alternative to EM-based solutions due to the biostability and energy-related requirements of this scenario. However, molecular signals suffer a significant amount of attenuation as they propagate through the medium, thus limiting the transmission range. In this paper, a signal amplification scheme for molecular communication nanonetworks is presented wherein a group of emitters jointly transmits a given signal after achieving synchronization by means of Quorum Sensing. By using the proposed methodology, the transmission range is extended proportionally to the number of synchronized emitters. An analytical model of Quorum Sensing is provided and validated through simulation. This model is the main contribution of this work and accounts for the activation threshold (which will eventually determine the resulting amplification level) and the delay of the synchronization process.

**Keywords** Amplification · Molecular Communication · Quorum Sensing · Synchronization · Nanonetworks · Bio-inspired

NaNoNetworking Center in Catalunya (N3Cat)
Universitat Politècnica de Catalunya
C/ Jordi Girona 1-3, 08034 Barcelona, Spain
Tel.: +34934017182
Fax: +34934017055
E-mail: {abadal,llatser,acabello}@ac.upc.edu and eduard.alarcon@upc.edu

## 1 Introduction

Nanotechnology enables the development of nanomachines, that is, devices in a scale ranging from one to a few hundreds of nanometers. These nanomachines are not just the downscaled version of classical devices, but the result of taking advantage of the unique properties of nanomaterials at this scale. For instance, novel nanosensors are able to detect the presence of virus and other harmful agents [17], or to sense chemical compounds in concentrations as low as one molecule [35].

Still, nanomachines are expected to be capable of performing very simple tasks due to their reduced size and energy constraints. Nanonetworks (i.e. networks consisting of nanomachines) are envisaged to extend the capabilities of single nanomachines in terms of complexity and range of operation [4]. For instance, Wireless NanoSensor Networks (WNSNs) [6] represent a particular case of nanonetworks in which nanosensor motes communicate in order to cover larger areas and reach unprecedented locations.

Numerous applications of WNSNs have been proposed in the biomedical, environmental, industrial and military fields [6]. Biomedical applications show best potential with respect to the unique characteristics of WNSNs, since the nanoscale is the natural domain of molecules, proteins or DNA sequences. Moreover, nanosensors may provide an interface between biological phenomena and electronic nanodevices. In *intra-body networks* [7], a group of nanosensors will gather data about the level of different substances or the presence of certain agents (e.g. cancer biomarkers) and will transmit it wirelessly to the macroscale. This way, *intra-body networks* are envisaged to provide ultra-accurate new health monitoring systems [7].

How nanomachines will communicate is still an important research challenge. Wireless electromagnetic communication, by means of graphene-based nano-antennas, has been proposed to address this issue [7,18,34]. These techniques are expected to produce ultra-high frequency radiation (in the THz range [19]), offering low propagation delays and high bandwidth. However, biomedical applications (and particularly *intra-body networks*) usually require the use of bio-compatible and non-invasive solutions. While the biological compatibility of EM-based techniques remains under study, their energy efficiency figures render impractical their use in such an energy-constraint scenario. These issues therefore compromise the suitability of electromagnetic communication in the biomedical scenario.

Instead, the research community is considering alternative communication paradigms that mimic the ones developed by nature. *Molecular communication* [32] is used by cells to communicate among them, and it encodes information into molecules that are released until they eventually reach the receiver, that is, the molecules are *physically* transported by means of diffusion to the receiver. The bio-compatibility of such communication technique is expected to be extremely high given its biologically inspired nature, enabling its employment for intra-body networks and other biomedical applications [4].

Molecular communication is based on completely different principles when compared to EM-based techniques, and therefore presents important challenges that require the design and development of radically new communication principles. For instance, the transmitted molecular signals suffer a great amount of attenuation and distortion as they propagate through the medium [32]. Since the molecule generation rate, reservoirs and emission capabilities of molecular transmitters are expected to be limited, the range of molecular communication is restricted to the very short range. Although amplification schemes are necessary in order to extend the transmission range and possibilities of molecular communication, little research has been conducted in this regard so far [25]. In [3], we presented a cooperative signal amplification technique especially tailored to the peculiarities of molecular communication and based on Quorum Sensing [12, 15, 2, 1]. In this paper, we extend the previous work by developing a mathematical framework, validated by means of simulation, which accounts for the amplification level and the delay of the amplification process. Nowadays, research efforts are devoted to *experimentally* validate the principles of both Molecular Communications and Quorum Sensing for communications at the nanoscale. We refer the interested reader to [5].

The remainder of the paper is organized as follows. Further details about molecular communication and its suitability for nanocommunication networks are introduced in Section 2. Next, the scalability problem that serves as motivation for this paper is formally stated in Section 3. The proposed amplification scheme is reviewed in Section 4 and analytically modeled in Section 5. After presenting and validating the model, some performance results are shown in Section 6 and the conclusions are presented in Section 7.

## 2 Background: Molecular Communication

Molecular communication is composed of three phases: emission, propagation, and reception (see Figure 1). In the first phase, emitters release molecules as a response to a certain command. On the receiver side, specific signal transducing mechanisms chemically react to concentrations of particles allowing the receiver to decode the message. Molecular transceivers needed for emission and reception of information are expected to be easy to integrate in nanodevices, as this new paradigm makes use of the same mechanisms that have been developed by nature for communication among cells inside the body. Moreover, the use of these chemically driven transceivers ensures the bio-compatibility of the process, as well as an extremely high energy efficiency [24].

The propagation process deals with the diffusion of molecules from the transmitter to the receiver through the medium. We consider that the space where the communication takes place contains a fluidic medium with a homogeneous concentration of molecules [30]. Under these conditions, communication molecules released by the emitters propagate through the medium by means of spontaneous diffusion [36]. In this case, the molecules move follow-

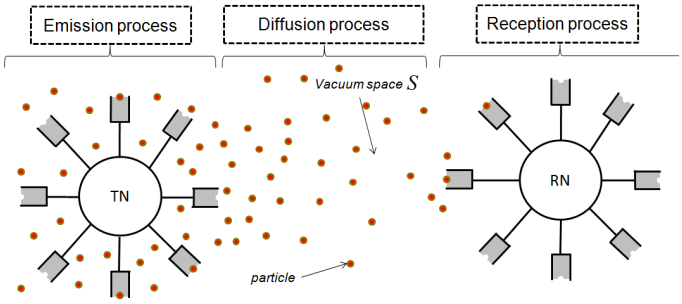


**Fig. 1** Processes present in diffusion-based molecular communication [30].

ing concentration gradients in a process that can be modeled using the Fick's laws of diffusion [29]. Several diffusion-based mechanisms have been identified in nature, both for short-range and long-range nanonetworks, namely, calcium signaling [27] and pheromonal communication [28], respectively.

In summary, molecular transmitters will transmit a message encoded in a variable concentration of *communication molecules* that will propagate towards the receiver by means of diffusion. Actually, experimental results led to the conclusion that cells can adopt modulation schemes similar to the traditional AM or FM techniques [26]. Since the complexity of nanomachines is expected to be very low, researchers are proposing simple modulation techniques, such as concentration-based ON-OFF modulations that encode information into pulses [13, 23]. In this context the receiver interprets low and high molecular concentrations as "absence" or "presence" of a pulse and decodes the information bit accordingly. The interested reader can find more information about molecular communication in [32].

## 3 Problem Statement

Let us consider the scenario of a WNSN deployed inside our body for healthcare purposes, and which makes use of molecular communication. Each sensor communicates with its peers, encoding the information into pulses of communication molecules which propagate through the environment by means of spontaneous diffusion. In classical sensor networks, when an event is detected it is sent to a special node called "sink". Communication with this node is essential so that the sensed event can be processed and analyzed. Moreover, WNSN sinks could also serve as a gateway to the macroworld [7].

However, recent results on the characterization of the physical channel of diffusion-based molecular communication show that encoding the information to be transmitted into pulses of molecules presents significant challenges [21]. Besides the addition of noise from several sources [31], these pulses suffer a great amount of attenuation, delay and distortion as they propagate through the medium (see Table 1). In particular, results show that the amplitude of a molecular pulse is inversely proportional to the third power of the transmission

**Table 1** Scalability of communication metrics in wireless EM and molecular channels [21]

| Metric | EM channel | Molecular channel |
|---|---|---|
| Pulse delay | $\Theta(r)$ | $\Theta(r^2)$ |
| Pulse amplitude | $\Theta(1/r^2)$ | $\Theta(1/r^3)$ |
| Pulse width | $\Theta(1)$ | $\Theta(r^2)$ |

[$r$: transmission distance]

distance $r$, $\Theta(1/r^3)$ [21]. Please note the difference with the scalability of classical EM techniques[1]: $\Theta(1/r^2)$. Ensuring the connectivity of the network with the sink under these conditions is an open challenge, as the transmission range of individual nanomachines is strongly limited by *(1)* these attenuation figures and *(2)* the finite nature of the molecule reservoirs and emission capabilities of the transmitter. This issue is usually referred to as "reachback problem" in traditional wireless sensor networks [16].

To exemplify the problem, we performed two simulations in which pulses two milliseconds long were transmitted, assuming a constant amplitude of 50000 particles. The receiver is located 10 micrometers away from the transmitter in the first case, whereas in the second simulation the receiver is situated at a distance of 25 micrometers. These simulations were realized using the N3Sim framework; further details about this simulator can be found in [22].

Figure 2 shows the evolution over time of the particle concentration received in these two different cases. While the pulse received in the first case can be easily distinguished, the pulse in the second receiver is highly attenuated and masked by the molecular noise. Consequently, only the first receiver will be able to clearly identify "low" and "high" levels of concentration and thus to decode the message. In other words, we will assume that a higher signal power yields lower bit error rates even though the molecular noise might not be AWGN [31]. In fact, one could argue that the levels of molecular noise should be evaluated after performing several transmissions, since molecules from previous transmissions could accumulate in the environment. In our case, we assume that the environment is practically infinite. Hence and considering a sufficiently large relaxation time between transmissions, the interference effect of previous transmissions can be neglected.

## 4 Cooperative Signal Amplification

As shown above, the attenuation introduced per unit of distance makes pulse-based molecular communication only feasible in the short range, since a large number of molecules, presumably below the emission capabilities of the transmitter, are required in order to reliably cover higher distances. These effects

[1] In this case, only free space electromagnetic radiation was considered.

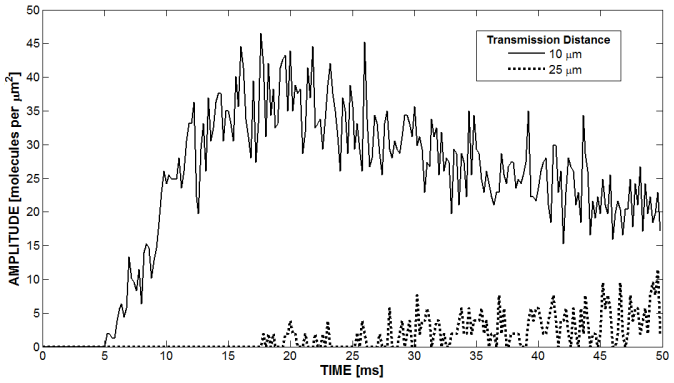


**Fig. 2** Reception of a pulse at distances of $10\mu$m (solid line) and $25\mu$m of the transmitter (dotted line).

may even render unfeasible the approach of nodes competing for the channel, traditionally used in current wireless networks. Instead, cooperative schemes where nodes coordinate and jointly transmit the same signal, amplifying it, may allow the implementation of diffusion-based molecular communication. The main challenge then is how to coordinate the action of a group of nanomachines to accomplish the cooperation desired. We propose Quorum Sensing [12] as a way to coordinate the emission of a group of transmitters so that higher distances can be covered while relaxing the power consumption constraints.

In the following, both the main principles of Quorum Sensing and the proposed amplification scheme are presented.

### 4.1 Quorum Sensing

Quorum Sensing is a biological process that enables the synchronization of a population of bacteria [15]. In order to synchronize with the group, each bacterium releases *synchronization molecules* at a constant rate. These molecules are called autoinducers since they trigger the release of more particles of the same kind when sensed by other bacteria. Hence, the concentration of *synchronization molecules* in the environment increases proportionally with the bacterial population. This way, bacteria are able to sense their population density by detecting the level of autoinducer concentration in their close environment. When this concentration reaches a critical *threshold*, the group responds with a synchronized population-wide change of behavior [12].

Quorum Sensing has been described as "the most consequential molecular microbiology story of the last decade" [20] since it is a highly widespread phenomena in the bacterial world. The reason behind this ubiquitous presence is considered to be evolutionary. Quorum Sensing enables the control of bacterial functions that are unproductive when undertaken by a single bacterium but become effective when undertaken by the group; processes that are generally crucial for the species survival. For instance, bacteria species commonly need

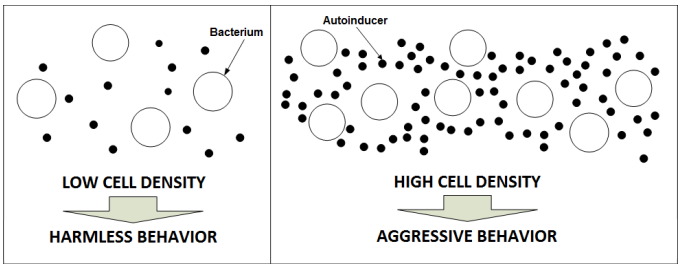


**Fig. 3** Quorum Sensing behavior for low and high cell densities.

to activate virulence factors in order to survive or spread. The host's defenses will easily deal with the outbreak of an individual bacterium, whereas the attack of a large group of bacteria will probably result in a successful infection. Many other examples of behaviors controlled by Quorum Sensing can be found in the literature: motility, DNA processing or bioluminescence, amongst others [15,38]. Further investigations have reported that some bacteria are able to distinguish between different types of autoinducers based on the chemical structure of such particles. In fact, some bacteria count on complex Quorum Sensing systems capable of concurrently reacting to different types of autoinducers sequentially or in parallel, constructively or destructively [15], enabling complex interactions between groups of bacteria and the environment.

The pervasive nature of Quorum Sensing has aroused the interest of the scientific community, which is dedicating considerable efforts to the theoretical analysis and modelling of Quorum Sensing from different perspectives [11,20, 14,5]. In our previous work, Quorum Sensing principles were analyzed from the communication perspective as a way to coordinate the course of action of several nanomachines by means of molecular communication, thus achieving global synchronization in a fully distributed manner [2]. Bacteria follow a rather simple algorithm with no need of configuration, two characteristics that might be critical when implementing Quorum Sensing functionalities in devices as limited in terms of complexity as nanomachines [1]. Moreover and as pointed out above, several Quorum Sensing schemes can be combined to potentially implement complex interactions between groups of nanomachines, making use of what has been called "Molecular Division Multiple Access" [28] to significantly expand the potential applications of these systems.

The existing characterization and analytical works in this field could be used for the experimental design and implementation of Quorum Sensing-enabled schemes [9,33]. Also, the creation of specific testbeds for Quorum Sensing, such as the MoNaCo project experimental platform [5], will enable the experimental validation of existing efforts, including the results presented next.

### 4.2 Proposed Amplification Scheme

In [3], we proposed the employment of Quorum Sensing to achieve signal amplification in diffusion-based molecular nanonetworks. Indeed, the Quorum Sensing process can be used so as to synchronize the course of action of a group of nodes that will jointly transmit pulses of molecules. This cooperative scheme is expected to provide a larger transmission range, as it allows the emission of amplified signals that will be able to reach distant receivers. As we will see in Section 6, the resultant transmission range will depend on the number of nodes considered.

The proposed scheme has two differentiated parts, which can be summarized as follows:

1. **Synchronization Phase:** firstly, when a node has information to transmit to other distant nodes (or to the sink in a WNSN scenario), it releases *synchronization molecules* at a constant rate in order to start a Quorum Sensing process with its surrounding neighbours. Adjacent nodes detect these *synchronization molecules* and start emitting molecules of the same type until its concentration surpasses the activation threshold. Eventually, a *transmission cluster* of approximately $N$ nodes activates at a similar time instant.
2. **Amplification Phase:** after this synchronization phase, the original transmitter and its neighbours will jointly and coordinately transmit a given message by using *communication molecules*. Since the channel can be considered linear if the molecular concentration is sufficiently low (see Section 5.2 for more details) the signal is effectively amplified.

While the specific information encoded into the synchronized signal is left out of the scope of this paper, it is worth to note that it can be either a pulse, or a (pre)configured sequence of pulses. The pulse information could be encoded in the chemical structure of the autoinducers used in the synchronization phase, in order to guarantee that all the nodes will transmit the same signal. Furthermore and since hundreds of different autoinducers (synchronization molecules) exist, different autoinducers could trigger different synchronized signals. Similarly to bacteria, we assume that nanomachines are capable of decoding the structure of the received molecules, therefore being capable of distinguishing among the different types of synchronization and communication molecules.

In the next section we present our main contribution: an analytical model of Quorum Sensing that accounts for the activation threshold and the synchronization delay, which enable the evaluation of several parameters of the amplification process, such as the level of amplification or its delay. This model is also validated by means of simulation, using the N3Sim framework [22].

## 5 Analytical Model of Quorum Sensing for Synchronization Purposes

In light of the principles explained in Section 4, we can define Quorum Sensing as a process by which a group of agents coordinates its behavior as a function of its population density. Generally, we can consider a given group of agents $\mathbb{S}$ deployed in a certain environment. Each of these agents will release specific *synchronization molecules* in a constant rate, causing an increase of the molecular concentration in the environment. Finally, these agents are capable of reacting when the concentration of these molecules reaches a certain threshold. While in the biological realm the agents are bacteria and they sense the autoinducer concentration to be aware of their cell density, in our case the agents will be molecular communication-enabled nodes that will use Quorum Sensing to perform cooperative signal amplification.

The objective of this section is to analytically derive the expression of the molecular concentration in a cluster $\mathbb{S}$ of N nodes that release molecules at a constant rate, as part of the Quorum Sensing routine. With this expression, we will be able to formally determine the mathematical dependence between the concentration of molecules in the environment and the node density. This way, we will extract, as a function of the node count:

1. An estimation of the molecular concentration above which a group of nodes should react (activation threshold).
2. The delay introduced by Quorum Sensing as a synchronization process.

We will follow an inductive reasoning. First, in Section 5.1, we will analyze the expression of the molecular concentration given by Bossert and Wilson [8] for a continuous and constant emission of molecules. In Section 5.2, we will derive the molecular concentration resulting from the aggregation of a group $\mathbb{S}$ of emitters, assuming certain conditions. After that, both the estimation of the activation threshold (Section 5.3) and the delay introduced by the synchronization phase (Section 5.4) will be calculated. All the expressions will be validated through simulations, using the N3Sim framework introduced earlier in this paper.

### 5.1 Individual Emission

Suppose $Q$ molecules are released by a node at a time $t = 0$ in a homogeneous environment of diffusivity $D$. The density $U$ in a point at distance $r$ at a certain instant $t$ is given by Roberts as [8]:

$$U(r,t) = \frac{2Q}{(4\pi Dt)^{\frac{3}{2}}} e^{-\frac{r^2}{4Dt}} \tag{1}$$

Taking this equation as a starting point, William H. Bossert and Eduard O. Wilson [8] expressed the density of molecules/autoinducers in the scenario of

a constant emission of autoinducers over time. The expression is the following:

$$U(r,t) = \frac{Q}{4D\pi r} erfc(\frac{r}{\sqrt{4Dt}}) \tag{2}$$

where $Q$ now refers to a constant emission rate in molecules per unit of time.

When a node performs a punctual emission, the released molecules diffuse away and the particle concentration in any given point progressively decreases over time. On the contrary, the particle concentration will monotonically increase in the continuous case (the one observed in Quorum Sensing), as the emitter is constantly releasing particles to the medium. However, there is an upper limit for the achievable particle concentration. If the source continues emitting for a long time, the density function will approach the value:

$$U(r) = \frac{Q}{4D\pi r} \tag{3}$$

which will be further used as a normalizing factor.

Figure 4 plots the normalized particle concentration over time at a distance of 1 $\mu$m from the emitter. The theoretic value of the particle concentration becomes independent of time in what can be considered as a permanent regime. Ideally, the flux of molecules entering any given volume in this situation is the same as the flux of outgoing molecules, thus stabilizing the value of the particle concentration. Mathematically, this effect is modeled by the asymptotic behavior of the complementary error function, whose Taylor series is:

$$erfc(z) = 1 - \frac{2}{\sqrt{\pi}} \sum_{n=0}^{\infty} \frac{(-1)^n z^{2n+1}}{n!(2n+1)} \tag{4}$$

and $z = \frac{r}{\sqrt{4Dt}}$ in our case.

In order to keep the model tractable, we assume that the nodes performing Quorum Sensing release molecules continuously and that the synchronization is accomplished under permanent regime conditions. The time value $t$ can be considered to be high, and thus the $z$ term will be close to zero. Hence, under permanent regime, the complementary error function can be approximated as a linear function:

$$erfc(z) \approx 1 - \frac{2z}{\sqrt{\pi}} \tag{5}$$

that can be introduced into Equation (2). As we can see in Figure 4, this approximation performs remarkably well when the time value $t$ is higher than a few milliseconds. The simulation data, obtained by analyzing the concentration sensed by a receiver located 1 $\mu$m away of a node emitting at a constant rate, matches both the theoretic value and the approximation.

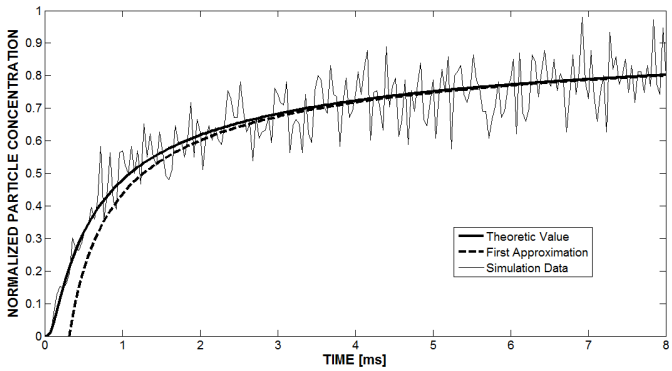


**Fig. 4** Simulation data, theoretic value and first approximation of the normalized particle concentration at a distance of $r = 1\mu m$ of a constant emitter

### 5.2 Autoinducers Accumulation

Let us now assume that the concentration of molecules in the environment is, at all times, sufficiently low so that the probability of collision between particles is negligible. Under this assumption and in a scenario devoid of external forces, we can consider that the diffusion-based molecular channel is linear. In [13], simulation results have shown that although molecular diffusion is governed by a nonlinear phenomenon, i.e., Brownian motion, the diffusion process has a linear behavior from a macroscopic perspective. Hence, we can apply the superposition principle, this is, the addition of two received emissions will yield the same signal than the reception of the addition of two emissions.

In the Quorum Sensing scenario, a given group $\mathbb{S}$ nodes is deployed randomly forming a cluster. Each of these nodes starts emitting synchronization molecules at some point, at a constant rate. Consistently with the reasoning pointed out above, we assume that the concentration of such synchronization molecules is low enough to consider the channel linear. Under these circumstances, it is possible to calculate the aggregated concentration of molecules at any point in space as the sum of the contributions of the group $\mathbb{S}$ of emitters. Employing the value of the maximum achievable concentration shown in Equation (3), and considering that each emitter is at a distance $r_i$ (i $\in \mathbb{S}$) of the evaluated point, we obtain:

$$U = \sum_{i \in \mathbb{S}} \frac{Q}{4D\pi r_i} = \frac{Q}{4D\pi} \sum_{i \in \mathbb{S}} \frac{1}{r_i} \tag{6}$$

Even though the nodes are expected to be randomly deployed, we assume now that the nodes are arranged in a perfect tridimensional grid so that the immediate neighbourhood of each node will be the same for all of them. This assumption helps to keep the model tractable without compromising its accuracy. The analytical results will be compared with simulation data in which

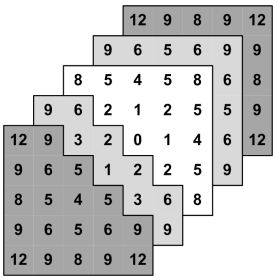


**Fig. 5** Squared normalized distances with respect to the central node, in a perfect tridimensional grid of five units of arista.

the nodes are randomly arranged, in order to show that the approximation performs well enough.

Following the perfect grid disposition, the node density $\rho$ will be constant over all the space and will only depend on the given distance between adjacent nodes $R$. For instance, a cube of $(MR)^3$ volume units will contain $N = M^3$ cells and thus, the resulting node density will be:

$$\rho = \frac{M^3}{(MR)^3} = \frac{1}{R^3} \tag{7}$$

Moreover, the euclidean distance between any given two nodes of the grid will be a proportional to $R$ (see Figure 5). In a perfect grid of N nodes (MxMxM), we can then calculate the particle concentration sensed by a node situated at any given point. For a node located at $(X_d, Y_d, Z_d)$, at an euclidean distance $d$ of the central node $(X_0, Y_0, Z_0)$, the particle concentration can be expressed as:

$$U(N,d) = \frac{Q}{4D\pi} \sum_{i \in \mathbb{S}} \frac{1}{r_i} = \frac{Q}{4D\pi R} \Phi(N,d) \tag{8}$$

where $\Phi(N,d)$ stands for the sum of the inverse of the normalized distances between the considered node and all the other nodes of the cluster:

$$\Phi(N,d) = \sum_i \sum_j \sum_k \frac{1}{\sqrt{|X_i - X_d|^2 + |Y_j - Y_d|^2 + |Z_k - Z_d|^2}} \tag{9}$$

Indexes $i$, $j$ and $k$ range from $-M/2$ to $M/2$ ($N = M^3$) and represent relative positions with respect to the central node, for each cartesian axis. Introducing the density equation (7) into Eq. (8) we obtain:

$$U(N,d) = \frac{Q}{4D\pi} \rho^{1/3} \Phi(N,d) \tag{10}$$

We can further treat this equation by introducing $\Phi(N,0)$ or "central aggregation factor", which accounts for the sum of the contributions of the N nodes to the central molecular concentration:

$$U(N,d) = \frac{Q}{4D\pi} \rho^{1/3} \Phi(N,d) \frac{\Phi(N,0)}{\Phi(N,0)} \tag{11}$$

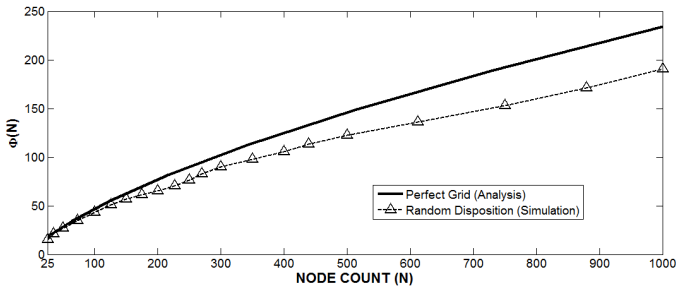


**Fig. 6** Central aggregation factor $\Phi(N)$ as a function of the number of nodes $N$.

The resulting $\frac{\Phi(N,d)}{\Phi(N,0)}$ term will be referred as attenuation factor or $\alpha(d)$, whereas $\Phi(N,0)$ can be simply expressed as $\Phi(N)$. Therefore:

$$U(N,d) = \frac{Q}{4D\pi}\rho^{1/3}\alpha(d)\Phi(N) \tag{12}$$

This last expression is quite intuitive and proves how the molecular concentration $U$ is proportional to the node disposition, which is modeled by the total number of nodes deployed $N$ and the node density $\rho$. While the molecular concentration is directly proportional to the node density, its dependence with the total number of nodes is modeled through the central aggregation factor $\Phi(N)$ (see Figure 6).

Therefore, a certain number of nodes $N$ will need to be deployed forming a cluster of density $\rho$ in order to reach a threshold concentration of autoinducers and thus to activate the whole colony, following the Quorum Sensing principles. The achievable concentration also depends on the nodes characteristics (emission rate $Q$) and the environment in which they are deployed (diffusion coefficient $D$).

Nevertheless, the concentration is not homogeneous as it depends on the distance $d$ to the central node. Specifically, the concentration slightly decreases as we approach the edges of the cluster. This centrality dependence of the molecular concentration is modeled by the position-related attenuation factor ($\alpha(d)$), the behavior of which is shown in Figure 7. The attenuation is low and almost constant at the core nodes, reaching only significant values in outer areas and a maximum attenuation of no more than 3 dB at the edge.

Finally, it is worth pointing out that the perfect node arrangement approximation performs remarkably well in light of the results shown in Figures 6 and 7, in which the theoretic values do not differ much from the simulation data.

### 5.3 Threshold Calculation

As previously discussed, nodes performing Quorum Sensing react upon sensing a concentration of autoinducers higher than a given level called *activation*

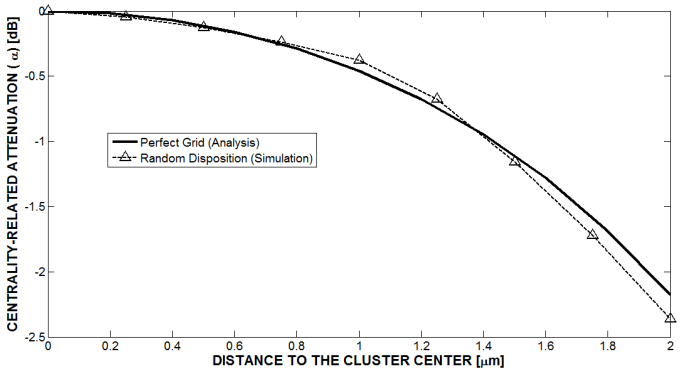


**Fig. 7** Position-dependent attenuation factor $\alpha$ as a function of the distance to the central node $d$ in a cluster of radius 2 $\mu$m.

*threshold*. These nanomachines will be randomly deployed in the targeted environment and are expected to be identical, thus having the same activation threshold. The choice of a reasonable value for this parameter is the key for the proper activation of nanodevices in the Quorum Sensing phase. For instance, the synchronization process will obviously fail if the activation threshold is set above the maximum achievable molecular concentration. Therefore, the threshold $K$ is should be lower than the value of $U_{max}$:

$$K < U_{max} = \frac{Q}{4D\pi}\rho^{1/3}\Phi(N) \tag{13}$$

which is, under the assumption of a perfect tridimensional grid, the concentration sensed at the central node.

Equation (13) sets the maximum value for the activation threshold in a cluster of node density $\rho$ consisting of $N$ nodes. However, the molecular concentration depends on the position of each node inside the cluster, as shown in the previous section. More specifically, the concentration decreases as we approach the edges of the cluster (see Figure 7). Therefore, the activation threshold determines the percentage of nanodevices of a cluster that will effectively synchronize: a low threshold will ensure an activation of 100% of the nodes of a given *transmission cluster*.

Nevertheless, an excessively low threshold compromises the quality of the transmission. As we will see in Section 6, the number of synchronizing nodes determines the maximum distance at which a message will be successfully decoded. *Transmission clusters* consisting of less than a certain number of nodes will not be able to reach receivers located at a given distance and should not activate due to molecular interference and energy consumption reasons. However, these clusters will still activate if the preset threshold is inappropriate.

### 5.4 Delay Calculation

Once the activation threshold $K$ for Quorum Sensing-enabled nodes is chosen, an approximation of the time needed to reach quorum can be calculated. If we use the first approximation shown in Equation (5), the concentration of autoinducers in a certain point in space can be expressed as:

$$U(r,t) \approx \frac{Q}{4D\pi} \sum_{i \in \mathbb{S}} \left[ \frac{1}{r} - \frac{1}{\sqrt{\pi D t}} \right] \tag{14}$$

Using Eq. (12), for a set consisting of a perfect grid of N nodes, we can obtain:

$$U(N,d,t) \approx \frac{Q}{4D\pi} \left[ \rho^{1/3} \alpha(d) \Phi(N) - \frac{N}{\sqrt{\pi D t}} \right] \tag{15}$$

Ideally, the nodes will activate when the concentration $U$ reaches or surpasses the threshold $K$. The time needed for this to happen $t_K$ can be approximately obtained from Equation (15), when $U = K$.

$$t_K(d) \approx \frac{Q^2}{16 D^3 \pi^3} \frac{N^2}{\left( U_{max} \alpha(d) - K \right)^2} \tag{16}$$

As previously stated, the threshold $K$ has to be necessarily below the maximum molecular concentration $U_{max}$. If we suppose that the threshold will be $K = kU_{max}$, with $k \in (0,1)$, the delay can be expressed as follows:

$$t_K(d) \approx \begin{cases} \frac{1}{D\pi} \left( \frac{1}{\rho^{1/3} \Phi'(N)} \right)^2 \frac{1}{\Delta U(d)^2} & k < \alpha(d) \\ \infty & k > \alpha(d) \end{cases} \tag{17}$$

where $\Delta U(d) = \alpha(d) - k$ will be further referred as "concentration margin". Also, the dependence with the number of nodes $N$ is solely modeled with the term $\Phi'(N) = \frac{\Phi(N)}{N}$, which accounts for the mean contribution of each node to the total molecular concentration.

Hence, the approximate delay introduced by the synchronization process is given by Equation (17), being known the diffusivity $D$, the total number of nodes $N$ deployed with a density $\rho$, and the concentration margin $\Delta U$. The delay is infinite in those areas in which the threshold is higher than the maximum achievable concentration, or $k > \alpha(d)$.

As the previous equation suggests, the delay is highly determined by the node distribution. The more densely clustered the nodes are deployed, the higher the $\rho$ factor will be, thus improving the delay performance. This seems consistent with the intuitive explanation: the distance between nodes will be shorter if they are densely deployed, thus reducing the time needed for the molecular concentration to reach a certain level. The node count $N$ also has influence upon the delay through the inverse of the mean individual contribution $\Phi'(N)$. Figure 8 shows that the contribution of each node to the overall molecular concentration diminishes as the node count grows, making the delay to increase accordingly.

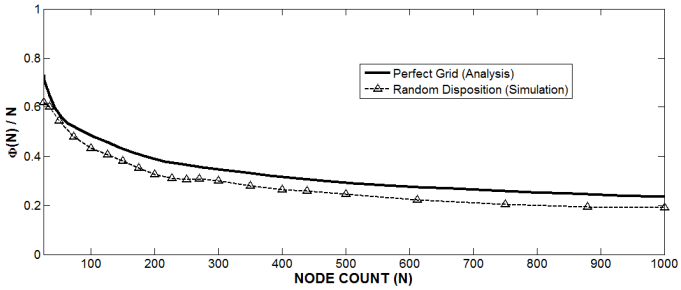


**Fig. 8** Mean individual contribution factor $\Phi'(N) = \frac{\Phi(N)}{N}$ as a function of the number of nodes $N$.

Secondly, the medium in which the nodes are deployed also affects the delay figures. In particular, the delay is inversely proportional to the diffusion coefficient $D$, as this parameter models how fast molecules diffuse away.

Finally, the delay depends on the activation threshold $K$ through the concentration margin term. In particular, the delay is inversely proportional to the square of the concentration margin $\Delta U(d)$, which represents the difference between the maximum attainable molecular concentration at a distance $d$ of the cluster center, and the chosen threshold level. In other words, the delay will be short as long as:

- The maximum attainable concentration is high. The delay will always be lower in central positions than closer to the edge of the cluster, as the molecular concentration decreases with distance (Figure 7). This effect explains the spatial dependence of the delay.
- The threshold is set to a low value. Figure 9 shows how lower thresholds imply shorter delays, due to the fact that the sensed molecular concentration needs less time to reach the activation level.

Since the position of the nodes inside the cluster is assumed random, the synchronization delay can be considered as a stochastic process dependent on the position of the considered node through the concentration margin parameter. Figure 9 shows both the mean value and standard deviation of the synchronization delay as a function of the chosen threshold. On the one hand, while the mean delay results may be considered large in absolute terms, one must take into account the delay in the propagation of molecular signals is considerably high if compared to electromagnetic communications. Therefore, the approach here presented could be still considered interesting in the molecular communication scenario. On the other hand, the variance of the delay could be seen as an indicator of the degree of synchrony of this molecular process. We can consider that synchronization with accuracy $\epsilon$ between N nodes is achieved if the maximum time differential between any two nodes is below the $\epsilon$ parameter. Statistically, the lower is the variance of the delay, the higher is the probability of meeting the synchronization condition with certain accuracy.

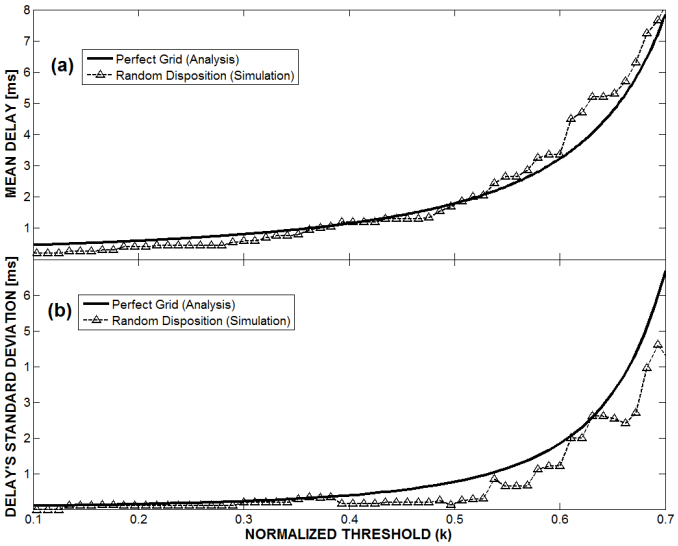


**Fig. 9** Synchronization mean delay $E[t_k(d)]$ and standard deviation $\sigma[t_k(d)]$ as a function of the chosen threshold.

Even though the results discussed above could lead to the conclusion that the preset activation threshold must be low so as to minimize the mean delay and the delay variance, an excessively low threshold compromises the quality of the transmission. As introduced in Section 5.3, the threshold must also take into account the target transmission range. A higher transmission range implies the need of a higher threshold which, in turn, entails a larger delay. We can conclude that the election of the activation threshold poses a design trade-off between performance in terms of amplification and in terms of delay, which needs to be inspected in future work.

## 6 Amplification Results

Recalling from Section 3, the amplitude of molecular pulses decreases proportionally to the third power of the transmission distance [21]. Thus, reaching certain distances using molecular communication schemes might result unfeasible, due to the energy constraints inherent to nanomachines. However, by employing Quorum Sensing, a group of nodes could coordinate their actions to transmit the same pulse synchronously [3] following the scheme reviewed in Section 4.2.

The model presented in Section 5 provides two fundamental expressions for the synchronization phase: activation threshold for a transmission cluster of $N$ nodes -Eq. (13)- and the delay introduced by this phase -Eq. (17)-. Whereas this section will focus on the amplification phase, more concretely on determining the improvement achieved in terms of transmission range.

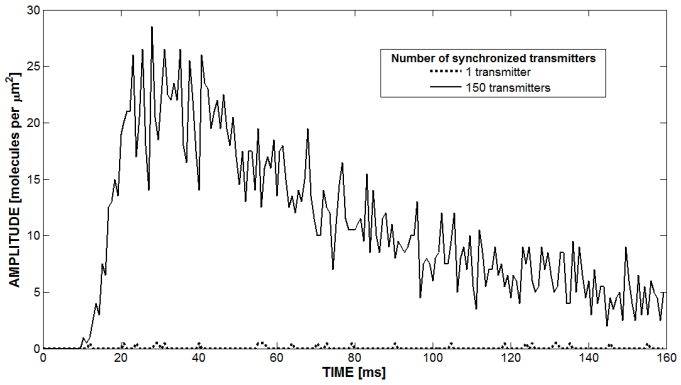


**Fig. 10** Reception, at a distance of 50 $\mu$m, of a pulse emitted by one transmitter (dotted line) and of a pulse amplified by a group of 150 transmitters (solid line).

To exemplify the validity of our proposed scheme, we performed two different simulations in which a single 2-millisecond long pulse is transmitted to a receiver located at a distance of 50 micrometers from the transmitter area. The pulse is transmitted by a single emitter in the first simulation, whereas a group of 150 emitters is the transmission source in the second simulation. Each emitter has an identical transmission power of 250 molecules per microsecond in either case. Figure 10 shows the evolution over time of the particle concentration received in these two different simulations. The receiver was only able to sense residual concentration of particles in the case of individual transmission, while the amplified pulse can be clearly identified in the second case. Eventually, the distant receiver will be able to successfully decode the molecular pulse if there is signal amplification at the source.

### Transmission Range

In [21], the amplitude of a molecular pulse in reception is calculated as the molecular concentration at the time instant at which the pulse reaches its maximum value, yielding:

$$c_{max} = \left(\frac{3}{2\pi e}\right)^{\frac{3}{2}} \frac{Q}{r^3} \tag{18}$$

Let us now assume the receiver is far enough of the transmission cluster so that the distance between the synchronized emitters is practically negligible with respect to the distance to the targeted receiver. In this case, we can consider a cluster of $N$ transmitters that transmit $Q$ particles each, as a punctual emitter that is releasing $NQ$ communication molecules. Previous work in [3] confirms, by means of simulation, that the amplitude of the received signal is proportional to the number of synchronized nodes.

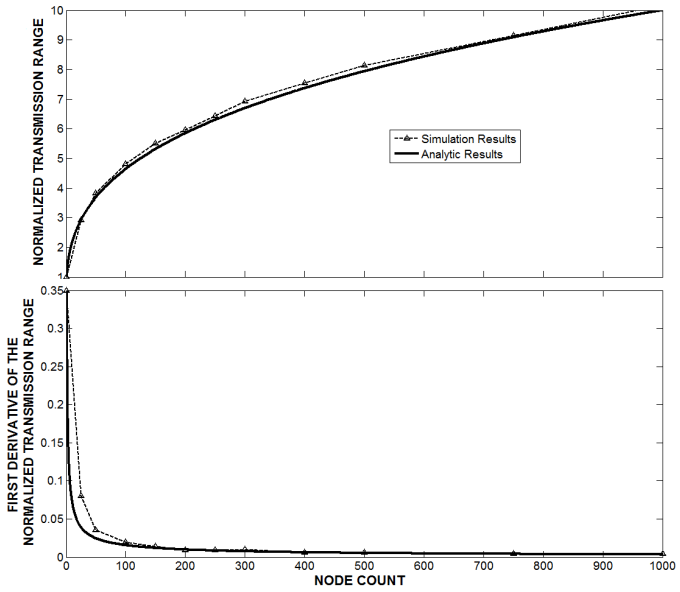


**Fig. 11** Normalized transmission range and its first order derivative as a function of the number of nodes used to amplify the signal.

If the receiver is at a distance $r$ and has a sensitivity of $c_S$, the number of emitters needed $N$ to reach the receiver can be calculated by solving the equation $c_{max,N} > c_S$:

$$N > \frac{c_S r^3}{Q} \left(\frac{2\pi e}{3}\right)^{\frac{3}{2}} \tag{19}$$

Hence, a transmission cluster of $N$ nodes emitting $Q$ molecules each, will be correctly received if a receiver of sensitivity $c_S$ molecules per volume unit is within a distance of:

$$r < r_{max} = \sqrt{\frac{3}{2\pi e}} \left(\frac{NQ}{c_S}\right)^{\frac{1}{3}} \tag{20}$$

and thus defining the transmission range $r_{max}$. If we consider the number of molecules per emitter $Q$ and the receiver sensitivity $c_S$ as preset constants, we can normalize equation (20):

$$\hat{r_{max}} = N^{\frac{1}{3}} \tag{21}$$

Figure 11 shows how the normalized transmission range scales as the number of synchronized emitters increases, as well as the behavior of its first order derivative. Both the analytic expression given by Equation (21) and the simulation results of previous work [3] are represented. As the transmission range is proportional to the cube root of the number of emitters used, both figures evidence a certain saturation of the amplification when the number of nodes

is high. Either way, the final transmission range will depend on the range of an isolated emitter, which can be approximately calculated by using Eq. (20) with $N = 1$.

Let us consider a transmitter capable of emitting 120 molecules per second [10] and a receiver with a sensitivity of 10 picomols [37] (equivalent to a concentration of $6.02 \cdot 10^{-3}$ molecules per $\mu$m$^3$). Under these conditions, the transmission range when emitting a 1-second pulse, will be:

$$r_{max} = \sqrt{\frac{3}{2\pi e}} \left( \frac{120}{6.02 \cdot 10^{-3}} \right)^{\frac{1}{3}} = 11.36 \ \mu m$$

Eventually, the transmission range can be enhanced by the cooperative amplification method depicted in this paper. For instance, a group of 125 emitters could reach distances of over 50 $\mu$m, whereas a group of 1000 emitters could be successfully received more than 100 $\mu$m away from the source.

## 7 Conclusions

Molecular signals suffer a significant amount of attenuation as they diffuse towards the receiver. In order to address this challenge, a cooperative signal amplification technique for molecular nanonetworks based on Quorum Sensing was proposed in previous work. In such cooperative scheme, the amplification level and, in turn, the final transmission range of the system will depend on the Quorum Sensing process.

In this paper, an analytical model of Quorum Sensing was provided and validated through simulation. Specifically, the model accounts for two fundamental figures:

*Activation threshold* Which has a direct influence to the number of nodes that will adequately activate and transmit the signal, as discussed in Section 5.3. Therefore, the transmission range that results from the amplification achieved will depend on the threshold chosen in the network dimensioning phase.

*Synchronization Delay* The downturn of the cooperative approach proposed in this paper is the delay that is added to the transmission. As shown in Section 5.4, both the mean value and the standard deviation of the delay introduced by the synchronization process increase almost exponentially with the threshold chosen. These results may be considered large in absolute terms, but they are commensurate with respect to the delay in the propagation of molecular signals, which is considerably high if compared to electromagnetic communications.

The results extracted from the analytical model evidence that there must be a compromise between level of amplification and delay. Low activation thresholds imply short synchronization delays, at the expense of not being able to guarantee high levels of amplification. On the other hand, a highly set activation threshold will result in larger transmission ranges, but also in larger delays.

## References


1. Abadal, S., Akyildiz, I.F.: Automata Modeling of Quorum Sensing for Nanocommunication Networks. Nano Communication Networks **2**(1), 74–83 (2011)
2. Abadal, S., Akyildiz, I.F.: Bio-Inspired Synchronization for Nanocommunication Networks. In: IEEE Global Telecommunications Conference (GLOBECOM 2011), pp. 1–5. Houston, TX, USA (2011)
3. Abadal, S., Llatser, I., Alarcón, E., Cabellos-Aparicio, A.: Quorum Sensing-enabled Amplification for Molecular Nanonetworks. to appear in 2nd IEEE International Workshop on Molecular and Nano-Scale Communications, held in conjunction with IEEE ICC (2012)
4. Akyildiz, I.F., Brunetti, F., Blazquez, C.: Nanonetworks: A new communication paradigm. Computer Networks **52**(12), 2260–2279 (2008). DOI 10.1016/j.comnet.2008.04.001
5. Akyildiz, I.F., Fekri, F., Forest, C.R., Hammer, B.K., Sivakumar, R.: MoNaCo: Molecular Nano-Communication Networks. URL http://www.ece.gatech.edu/research/labs/bwn/monaco/index.html
6. Akyildiz, I.F., Jornet, J.M.: Electromagnetic wireless nanosensor networks. Nano Communication Networks **1**(1), 3–19 (2010). DOI 10.1016/j.nancom.2010.04.001
7. Akyildiz, I.F., Jornet, J.M.: The Internet of nano-things. Wireless Communications, IEEE **17**(6), 58–63 (2010)
8. Bossert, W.H., Wilson, E.O.: The analysis of olfactory communication among animals. Journal of theoretical biology **5**(3), 443–69 (1963)
9. Danino, T., Mondragón-Palomino, O., Tsimring, L., Hasty, J.: A synchronized quorum of genetic clocks. Nature **463**(7279), 326–30 (2010). DOI 10.1038/nature08753
10. Devreotes, P., Derstine, P., Steck, T.: Cyclic 3', 5'AMP relay in Dictyostelium discoideum. The Journal of cell biology **80**(2), 291–299 (1979)
11. Dockery, J.D., Keener, J.P.: A mathematical model for quorum sensing in Pseudomonas aeruginosa. Bulletin of Mathematical Biology **63**(1), 95–116 (2001). DOI 10.1006/bulm.2000.0205
12. Fuqua, C., Winans, S., Greenberg, P.: Quorum Sensing in Bacteria: the LuxR-LuxI Family of Cell Density-Responsive Transcriptional Regulatorst. Journal of Bacteriology **176**(2), 269–275 (1994)
13. Garralda, N., Llatser, I., Cabellos-Aparicio, A., Pierobon, M.: Simulation-based Evaluation of the Diffusion-based Physical Channel in Molecular Nanonetworks. Proc. of the 1st IEEE International Workshop on Molecular and Nano Scale Communication (MoNaCom), held in conjunction with IEEE INFOCOM (2011)
14. Goryachev, A.B., Toh, D.J., Wee, K.B., Lee, T., Zhang, H.B., Zhang, L.H.: Transition to quorum sensing in an agrobacterium population: A stochastic model. PLoS Computational Biology **1**(4), 265–275 (2005)
15. Henke, J., Bassler, B.: Bacterial social engagements. Trends in Cell Biology **14**(11), 648–656 (2004)
16. Hong, Y.W., Scaglione, A.: Time synchronization and reach-back communications with pulse-coupled oscillators for UWB wireless ad hoc networks. In: Proceedings of the IEEE Conference on Ultra Wideband Systems and Technologies, pp. 190–194. Ieee (2003). DOI 10.1109/UWBST.2003.1267830
17. Hsiao-Yun Yeh: Real-time molecular methods to detect infectious viruses. Seminars in cell developmental biology **20**(1), 49–54 (2009)

18. Jornet, J.M., Akyildiz, I.F.: Graphene-based nano-antennas for electromagnetic nanocommunications in the terahertz band. In: EUCAP (ed.) Proc. of 4th European Conference on Antennas and Propagation. Barcelona (2010)
19. Jornet, J.M., Akyildiz, I.F.: Channel Modeling and Capacity Analysis for Electromagnetic Wireless Nanonetworks in the Terahertz Band. IEEE Transactions on Wireless Communications **10**(10), 3211–3221 (2011)
20. Krasnogor, N., Gheorghe, M., Terrazas, G., Diggle, S., Williams, P., Camara, M.: An appealing computational mechanism drawn from bacterial quorum sensing. Bulletin of the EATCS **85**, 135–148 (2005)
21. Llatser, I., Alarcón, E., Pierobon, M.: Diffusion-based Channel Characterization in Molecular Nanonetworks. In: Proc. of the 1st IEEE International Workshop on Molecular and Nano Scale Communication (MoNaCom), held in conjunction with IEEE INFOCOM (2011)
22. Llatser, I., Pascual, I., Garralda, N., Cabellos-aparicio, A., Pierobon, M., Alarcón, E., Solé-Pareta, J.: Exploring the Physical Channel of Diffusion-based Molecular Communication by Simulation. In: IEEE Global Telecommunications Conference (GLOBECOM 2011), pp. 1–5. Houston, TX, USA (2011)
23. Mahfuz, M.U., Makrakis, D., Mouftah, H.T.: On the characterization of binary concentration-encoded molecular communication in nanonetworks. Nano Communication Networks **1**(4), 289–300 (2010). DOI 10.1016/j.nancom.2011.01.001
24. Moore, M., Enomoto, A., Nakano, T., Okaie, Y., Suda, T.: Interfacing with nanomachines through molecular communication. IEEE International Conference on Systems Man and Cybernetics pp. 18–23 (2007)
25. Nakano, T., Shuai, J.: Repeater design and modeling for molecular communication networks. 1st IEEE International Workshop on Molecular and Nano Scale Communication (MoNaCom), held in conjunction with IEEE INFOCOM pp. 501–506 (2011)
26. Nakano, T., Suda, T.: Molecular communication through gap junction channels: System design, experiments and modeling. 2nd Bio-Inspired Models of Network, Information and Computing Systems pp. 139–146 (2007). DOI 10.1109/BIMNICS.2007.4610100
27. Nakano, T., Suda, T., Moore, M., Egashira, R., Enomoto, A., Arima, K.: Molecular communication for nanomachines using intercellular calcium signaling. In: Proceedings of the Fifth IEEE Conference on Nanotechnology, pp. 478–481. Citeseer, Nagoya, Japan (2005)
28. Parcerisa, L., Akyildiz, I.F.: Molecular Communication Options for Long Range Nanonetworks. Computer Networks **53**(16), 2753–2766 (2009)
29. Philibert, J.: One and a Half Century of Diffusion: Fick, Einstein, Before and Beyond. Diffusion Fundamentals **4**(6), 1–19 (2006)
30. Pierobon, M., Akyildiz, I.F.: A Physical End-to-End Model for Molecular Communication in Nanonetworks. IEEE Journal on Selected Areas in Communications (JSAC) **28**(4), 602–611 (2010)
31. Pierobon, M., Akyildiz, I.F.: Diffusion-based Noise Analysis for Molecular Communication in Nanonetworks. IEEE Transactions on Signal Processing **59**(6), 2532–47 (2011)
32. Pierobon, M., Akyildiz, I.F.: Information capacity of diffusion-based molecular communication in nanonetworks. Proc. of IEEE INFOCOM Miniconference pp. 2–6 (2011)
33. Prindle, A., Samayoa, P., Razinkov, I., Danino, T., Tsimring, L.S., Hasty, J.: A sensing array of radically coupled genetic 'biopixels'. Nature **481**(7379), 39–44 (2012). DOI 10.1038/nature10722
34. Rutherglen, C., Burke, P.: Nanoelectromagnetics: circuit and electromagnetic properties of carbon nanotubes. Small (Weinheim an der Bergstrasse, Germany) **5**(8), 884–906 (2009). DOI 10.1002/smll.200800527
35. Schedin, F., Geim, A.K., Morozov, S.V., Hill, E.W., Blake, P., Katsnelson, M.I., Novoselov, K.S.: Detection of individual gas molecules adsorbed on graphene. Nature materials **6**(9), 652–5 (2007). DOI 10.1038/nmat1967
36. Suda, T., Moore, M., Nakano, T., Egashira, R., Enomoto, A.: Exploratory research on molecular communication between nanomachines. In: in Genetic and Evolutionary Computation Conference (GECCO). Late Breaking Papers, June (2005)
37. Ugalde, U.: Autoregulatory signals in Mycelial Fungi. The Mycota **1**(2), 203–213 (2006)
38. Xavier, K., Bassler, B.: LuxS quorum sensing: more than just a numbers game. Current opinion in microbiology **6**(2), 191–197 (2003)